SYSTEM IDENTIFICATION & DAMAGE ASSESSMENT OF STRUCTURES USING OPTICAL TRACKER ARRAY DATA

Chin-Hsiung Loh[1,*] and Chuan-Kai Chan [1]
[1] Department of Civil Engineering, National Taiwan University
Taipei 10617, Taiwan.*Email:lohc0220@ccms.ntu.edu.tw

ABSTRACT

Damage assessment of a steel structure involves acquiring and identifying dynamic characteristics of the structure and using these characteristics to evaluate behavior and performance. To ensure the objective assessment three major issues need to be developed: sensing system, system identification and feature extraction. In this study, a unsymmetrical 3-story steel structure (fabricated with one week column in the first floor) subjected to a series of earthquake excitations with increasing level of excitation back to back. In between the earthquake excitation white noise excitation was also applied. Both the traditional sensing system (accelerometer and LVDT) and the optical tracker system were implemented in the structure to collect the vibration-based responses. First, the traditional system identification using global response data is used (subspace identification) to extract system natural frequencies and mode shapes from different set of seismic responses. Besides, to evaluate whether optical tracker array data from local measurement could be used to identify deterioration or damaged-induced changes in damage assessment, principal component analysis was applied to extract the curvature ad the earthquake–induce local stress of the structural member. From which the local stress distribution from different seismic event can be estimated. The relationship among the local displacement profiles, stress distributions and the global dynamic characteristics of the structure are investigated. The results reveal that the local flexibility was an excellent objective for both local and global condition assessment. Finally, discussion on the identified global dynamic characteristics from global measurement in relating to the calculated structural integrity index using optical sensing array data and local element strain on the identification of damage severity are presented.

KEYWORDS

Optical sensor, signal processing, damage detection, principal component analysis, null-space damage index.

INTRODUCTION

Structural health monitoring for systems involve three major key levels as defined: Leveel-1: detect the existing of damage; Level-2: detect and locate the damage; Level-3: detect, locate and quantify damage. To reach these three major levels sensing system, signal processing and feature extraction techniques play a very important rule. For sensing system, generally, to monitor the civil infrastructure during earthquake excitation accelerometers are the most common sensors to collect the vibration signals from the vibration of the structures. With the developed system identification techniques structural natural frequencies, damping ratios and mode shapes can be identified using acceleration data from global monitoring view point. To detect the damage location as well as damage severity usually requires data from multiple sensors (or dense sensor array) on some specific local area of the structure. Sensors such as strain gage, FBG or PZT can be used as a sensing array to collect the vibration data from a specific local area.

The research objective of this paper is to identify the local damage features from the vibration-based measurement of a reinforced concrete frame and a 3-story steel frame subjected to base excitation. With the availability of high resolution distributed sensing system, optical tracker on light targets, the damage features as well as the damage severity can be identified. Correlation of the local damage in relating the global damage features extracted from traditional instrumentation was discussed.

STRUCTURAL DESCRIPTION AND INSTRUMENTATION

Two different types of structural models are designed and tested in NCREE shaking table: one is the two-bay one story RC frame and the other one is the 3-story steel frame. Both structures were subjected to shake table test with different intensity level from the base.

The test specimen of RC frame was a one-storey two-spanned RC frame with an overall height of 2 m, and an approximate weight of the frame was 6454 kg. The frame consisted of a T-beam of 4.7 m × 0.7 m, as well as 3 columns with cross-section dimension of 20 cm × 20 cm. To catch the global behavior of the dynamic response of the frame, a total of four specimens were constructed with the same design details. The specimen was subjected to a single direction excitation. For the shake table test, 12 accelerometers were used to measure the acceleration response (*Figure 1*) and four lateral LVDTs (Linear Variable Differential Transformers) were instrumented to acquire displacement response. The sampling frequency for above devices is 200Hz. o collect the local dynamic response, Twenty-four optical sensors (the sampling frequency = 100Hz) were also instrumented on the central column for the acquisition of displacement information. The OPTOTRAK® Certus (as shown the number in *Figure 2*) was selected as the optical tracker which can tract the light source from 24 targets attached on the specimen. At both end of the center column, a dense optical array sensor is deployed in grid size (5cm x 20cm). The spatial dynamic displacement data is collected from the optical sensing system which consists of two major devices. One is the Target-based Photogrammetry that provides the ability to conduct dynamic measurement functions. The other device is OPTOTRAK® Certus which is the full 3-D optical tracker. It can track the optical laser flashed by the target system that marks on the specific points of the structure. The tracker has the ability to track how these three dimensional measurements change over time for dynamic motion measurement with RMS accuracy up to 0.1 mm. The size of the target is small enough so that it can placed in an network array.

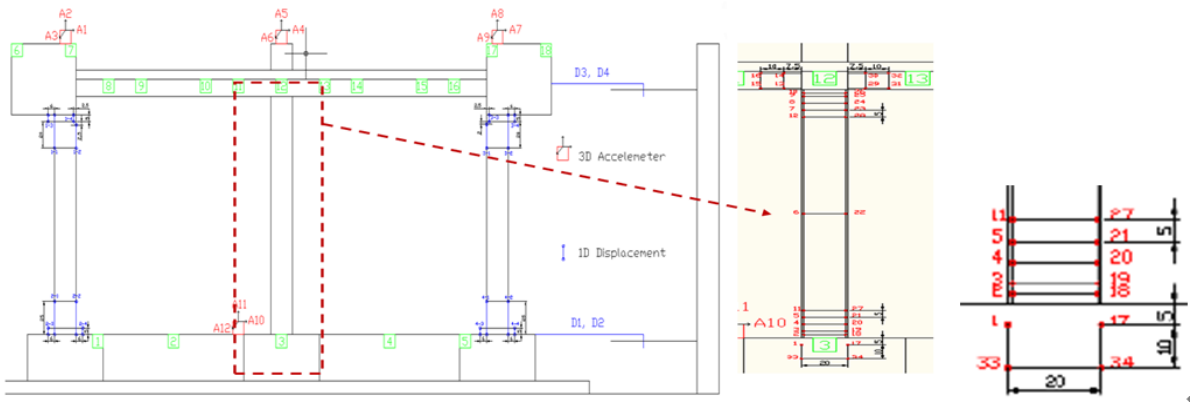

Figure 1 Different types of instruments on the test specimen including.
The optical sensing system is distributed on the central column.

Figure 2 Optical sensing system; (a) target (light source); (b) optical tracker;

The other test specimen is the two 3-story 350 cm in height steel structures, Specimen 1 and Specimen 2 respectively. The two steel structures are constructed with the same member size except Specimen 2 in which one column in the first floor (i.e. column at the north-west corner designed with smaller web thickness). Therefore, specimen 1 is a symmetric structure while specimen 2 is an anti-symmetric structure. The floor area is 1.5 m x 1.1 m. The total weight of each structure is 2.94 ton (include additional 0.5 ton on each floor). Three different types of instrumentation were used to collect the vibration response of the structure: accelerometer, LVDT and NDI optical tracker. The distribution of accelerometer and the LVDT is shown in *Figure 3a*. Detail description of NDI optical tracker is shown in *Figure 3b*. Due to the limitation of measurement technique only two columns of the first floor of specimen 2 are installed with the NDI measurement system. The spectrum compatible acceleration record (from Ch-Chi earthquake station TCU071) is used as the desired base excitation of the shaking table. The test protocol for the RC frame and the two steel structures are shown in *Table 1a* [Loh et al. 2011] *and 1b*, respectively**.** For the testing of steel structures the base excitation is arranged back to back

with different input intensity level. In between the earthquake excitation white noise excitation (with peak acceleration of 50 gal) was also applied to serve as the reference state of the structure before and after each earthquake excitation. In these experiments all the response measurement is with 200 Hz sampling frequency.

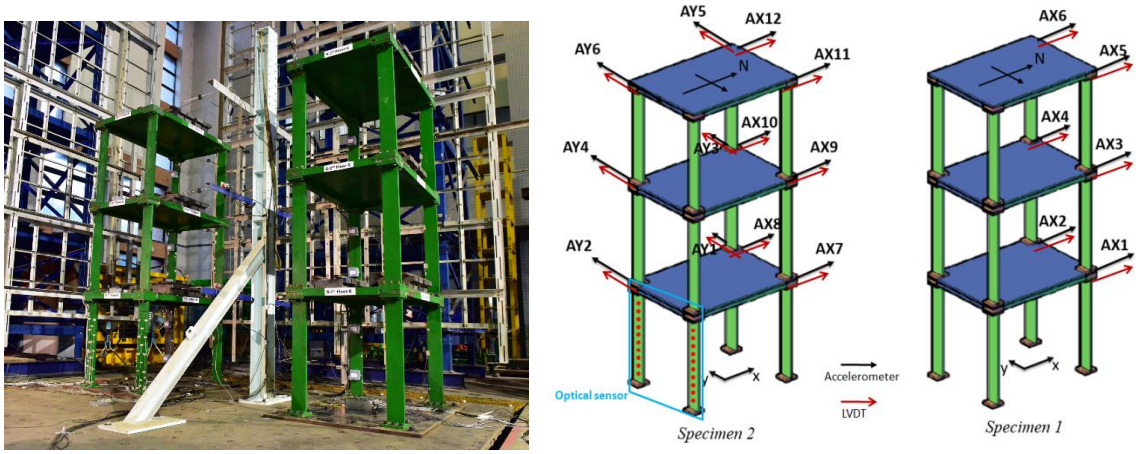

Figure 3a Photo of the two structures on shaking table, and the instrumentation of accelerometer and LVDT in the two structures.

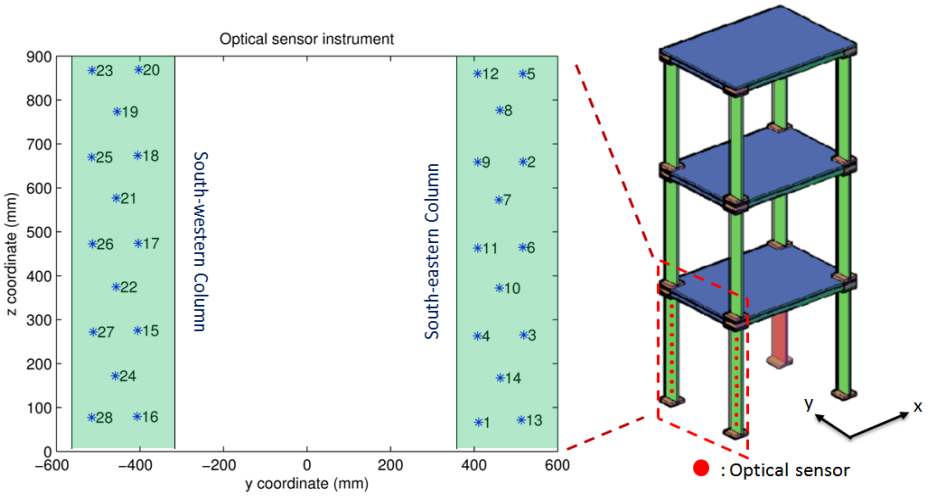

Figure 3b Distribution of optical sensors on the two columns of the 1st floor of Specimen 2

Table 1a Physical parameters measured or identified from the shake table tests of RC frame.

Specimen No.	Excitation	PGA (gal)	Max. Absolute Accel. (gal)	Max. Inter-Story Drift Ratio (%)
RCF6	White Noise	29	24	0.06
	Earthquake	**622**	**750**	**1.35**
	White Noise	30	15	0.04
RCF2	White Noise	27	41	0.02
	Earthquake	**815**	**1241**	**2.43**
	White Noise	30	28	0.05
RCF4	White Noise	29	46	0.03
	Earthquake	**1157**	**1305**	**3.29**
	White Noise	32	25	0.06
RCF3	White Noise	24	40	0.04
	Earthquake	**1287**	**1216**	**4.46**
	White Noise	35	25	0.06

Table 1b test protocol of two steel frames.

Run Num.	Ground motion(gal)		Direction	Test ID
Run 01	White noise 1	50	x	WN1
Run 02	White noise 2	50	x	WN2
Run 03	Earthquake1	95	x	EQ1
Run 04	White noise 3	50	x	WN3
Run 05	Earthquake 2	269	x	EQ2
Run 06	White noise 4	50	x	WN4
Run 07	Earthquake 3	400	x	EQ3
Run 08	White noise 5	50	x	WN5
Run 09	Earthquake 4	572	x	EQ4
Run 10	White noise 6	50	x	WN6
Run 11	Earthquake 5	674	x	EQ5
Run 12	White noise 7	50	x	WN7
Run 13	Earthquake 6	858	x	EQ6
Run 14	White noise 8	50	x	WN8
Run 15	Earthquake 7	994	x	EQ7
Run 16	White noise 9	50	x	WN9
Run 17	Earthquake 8	1190	x	EQ8
Run 18	White noise 10	50	x	WN10
Run 19	Earthquake 9	1329	x	EQ9
Run 20	White noise 11	50	x	WN11

LOCAL FEATURE EXTRACTION USING NDI DATA

To extract the local features from the 3-dimensional optical tracker distributed on the local structural member, the principal component analysis (PCA) was applied to reduce the data and extract the major principal components [Jolliffe, 2002]. With is technique and applied to the NDI data collected from the seismic response of 2-bay one story RC frame and a 3-story steel frame structure.

Analysis of 2-bay One Story RC Frame

Based on the NDI data collected from the central column of the 2-bay RC frame during the shaking tabled test, Figure X plots the distribution of the first four major principal vales of the four specimen. It is observed that the singular values of the first 3 PCs contribute over 99% of the entire signal. The 1st PC is a rigid-body motion, the 2nd PC is a shear deformation, and the 3rd PC is a bending-like deformation for the RC specimens. *Figure 4* shows the singular value distribution of all cases, and we can see that the more intense the excitation is, the less singular value the 1st PC (rigid body motion) contributes. Since the rigid body motion of a structure does not cause damage for a structure, therefore, the less the contribution of the rigid body motion is the more severe the damage may be. *Figure 5* shows the first 3 PCs of RC specimen RCF 6 and RCF 2. To analyze the stress/strain induced by ground shaking in the column, the rigid body mode needs to be removed. Since very dense optical sensors are distributed at the top and bottom of the center column with grid arrangement (or block arrangement), the average strain for each block can be calculated [Chao et al. 2013]. *Figure 6* shows the comparison of the calculated shear strain (γ_{xy}) of each block from each test specimen. the results show that larger shear strain was observed for RCF3 specimen which is consistent with the excitation level. Besides, the block axial strain can also be calculated:

$$\varepsilon_{yy} = \frac{\left(Ly_{1,d} - Ly_{1,0}\right) + \left(Ly_{2,d} - Ly_{2,0}\right)}{\left(Ly_{2,d} - Ly_{2,0}\right)} \tag{1}$$

where L is the length and width of the block and the suffix d and 0 represent the deformed state and original state of the block. Since ε_{yy} was calculated from each block the curvature of the column can be estimated by using $\kappa = (\varepsilon_1 - \varepsilon_2)/h$ to estimate the curvature in which ε_1 and ε_2 indicate the axial strain calculated from blocks in the central column. Since the test specimen was a one-story frame, which can be regarded as a simplified cantilever beam. A deformed cantilever beam divided into several segments and the displacement is mainly caused by the slope induced from the curvature near the fix end, and the curvature near the free end is close to zero, as shown in *Figure 7*. As a result, one can calculate the displacement caused by each segment and the accumulated slope from the curvature near the fix end. Thus, we can get the deformation of the frame. Comparison on the frame lateral displacement using NDI data (indirect estimation) and using LVDT (direct measurement) is shown in *Figure 8*. Good agreement was observed.

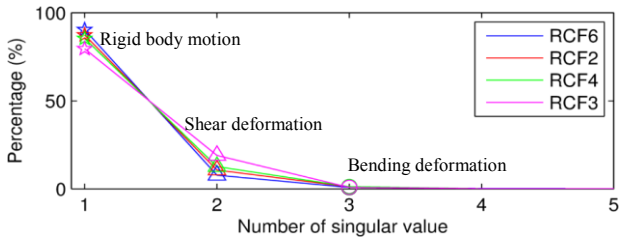

Figure 4 Distribution of singular values from PCA of NDI data of four RC specimens.

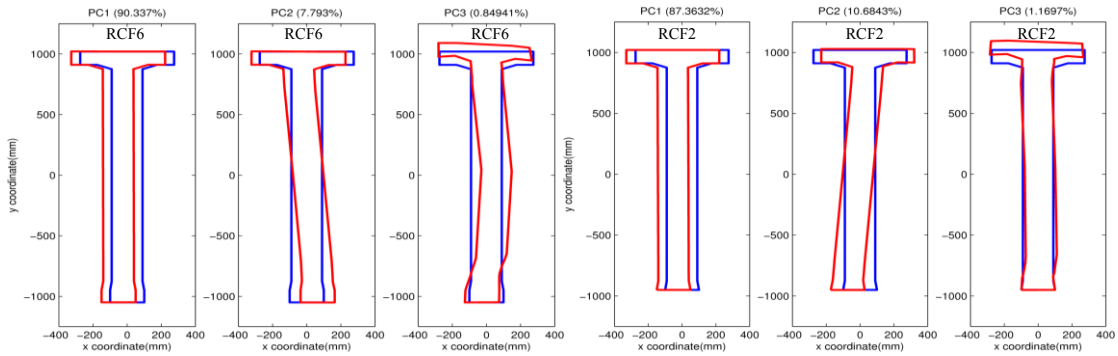

Figure 5 Plot the major three principal components of specimen RCF6 and RCF 2.

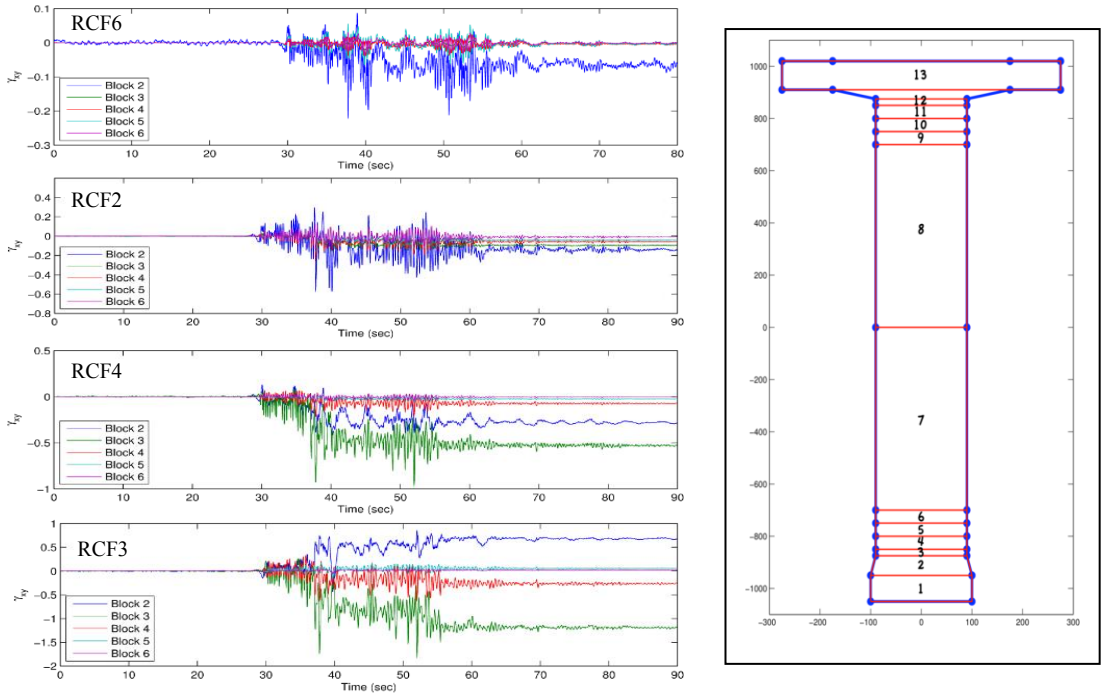

Figure 6 Plot the estimated shear strain of each block element from four test specimen.

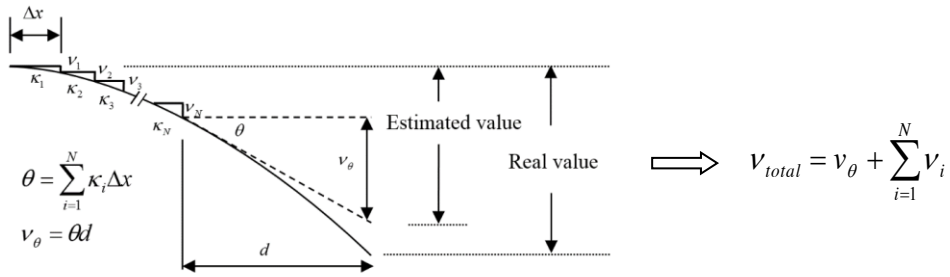

Figure 7 Estimate lateral displacement of a cantilevel beam using curvature-displacement relationship.

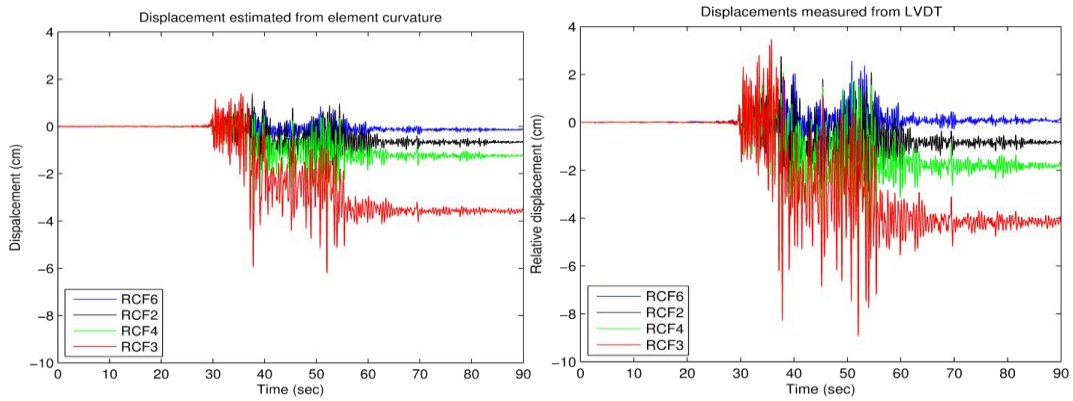

Figure 8 Comparison on the frame lateral displacement using NDI data indirect estimation (left) and using LVDT direct measurement (right)

Analysis of 3-story Steel Frame

An optical sensing system (NDI-Optical tracker) with 28 light sources was installed on the two columns of the first floor of Specimen 2. The optical tracker can detect the 3-D displacement of each light source which can provide the information for the identification of local member property during earthquakes. The measured data set is firstly arranged in data matrix to perform the principal component analysis (PCA). *Figure 9* shows the

extracted four principal components (PC) of the two columns. According to the results from PCA, the 1st PC belongs to the rigid body motion. Reconstruct the data matrix without 1st PC, one can obtain the deformation response of the columns. This extracted column deformation can be used to identify the stress distribution along the monitor column from each seismic excitation.

It is assumed that the deformed shape $v(z)$ of the column can use the 3rd-order polynomial (i.e. bending moment *M(x)* along the column height is assumed as a 1st-order polynomial) to fit the measurement under the assumption of linear static deformation theory. Based on the discrete monitoring NDI data, the continuous deformation $v(z)$ of the column can be obtained (this is under the assumption of the response of an equivalent linear system). The deformed shape of the column, for case of EQ6 loading, is fit by a 3rd-order polynomial and plotted as the green line in *Figure 10*. Then the stress distribution along the column height can be obtained from the deformed shape of the column:

$$\sigma(z) = \frac{M(z)}{I} h = hE \frac{dv^2(z)}{dz^2} \tag{2}$$

where z is the height of the column and *h* is the thickness of the column. By taking double differentiation of the deformation function, one can get the moment function $M(x)$. In this study, the numerical differentiation is employed, which is defined as [Boashash, 1992]*:*

$$\theta'(k) = \begin{cases} \frac{1}{12} \times (-25\theta(k) + 48\theta(k+1) - 36\theta(k+2) + 16\theta(k+3) - 3\theta(k+4)) & for \quad k = 1,2 \\ \frac{1}{12} \times (\theta(k-2) - 8\theta(k-1) + 8\theta(k+1) - \theta(k+2)) & for \quad k = 3,...,N-2 \\ \frac{1}{12} \times (25\theta(k) - 48\theta(k-1) + 36\theta(k-2) - 16\theta(k-3) + 3\theta(k-4)) & for \quad k = N-1, N \end{cases} \tag{3}$$

Figure 11 shows the distribution of earthquake-induced stress along the column for case of EQ2 (250 gal) and EQ5 (700 gal). A36 steel was used to construct the structure and the yield stress of the steel column is 275 Mpa. The column size is with cross section of 0.15 m × 0.025 m and the moment of inertia is 1.9531e-7 m^4. With these data one can estimate the stress at any location of the column. *Figure 12* plots the estimated maximum stress at the top of the column with respect to different level of earthquake base excitation (under the assumption of equivalent linear system). It is observed that the column stress exceed the yield stress when the excitation exceed pga>400 gal (after the test case of EQ3).

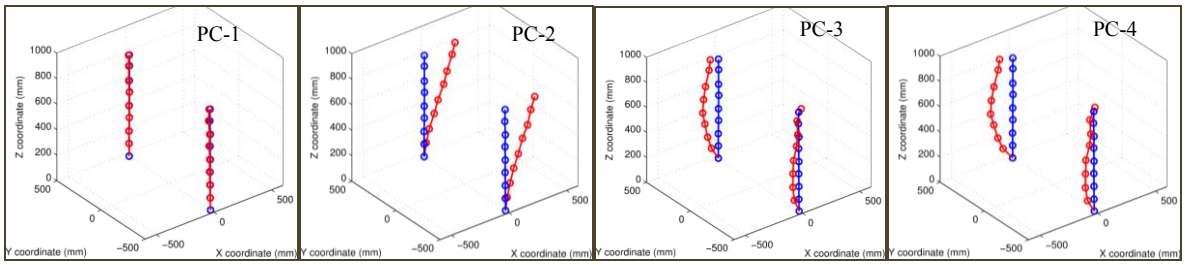

Figure 9 Identified four major principal components from NDI data of 3-story steel frame.

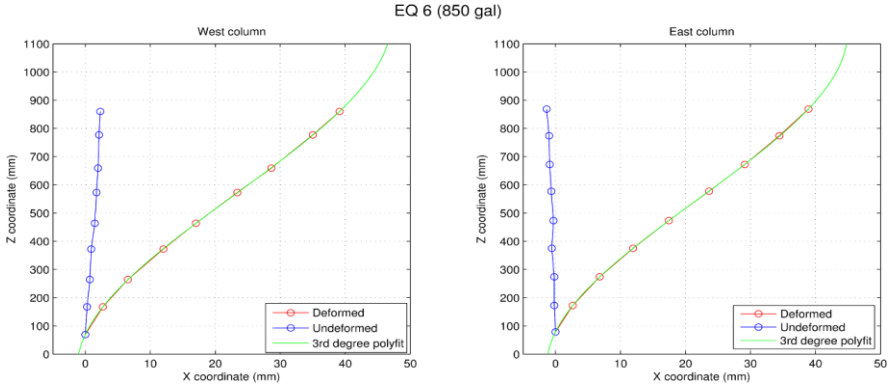

Figure 10 Deformed shape of two column under the case of EQ6 loading.

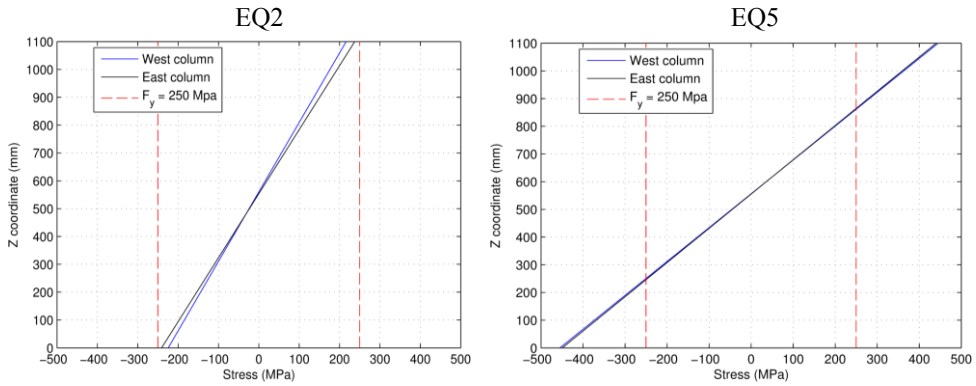

Figure 11 Identified stress distribution along the column height for case of EQ@ and EQ5 loading.

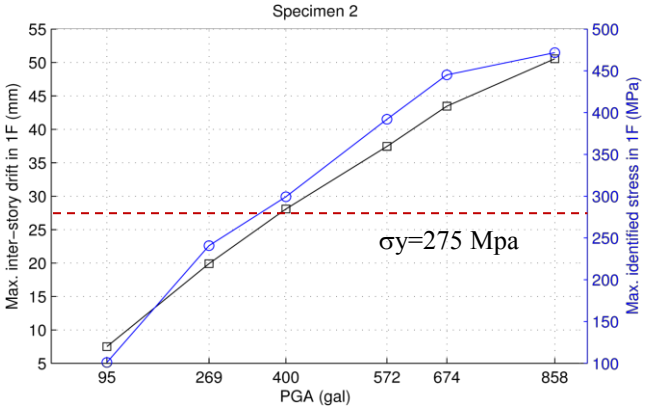

Figure 12 Plot the identified maximum stress at the top of the 1st floor column and the max. inter-story drift.

CORRELATIONS OF LOCAL PROPERTIES WITH GLOBAL DYNAMIC CHARACTERISTICS

Two-bay One-story RC Frame

Comparison on the calculated block strain (axial strain ε_{yy} and shear strain γ_{xy} from the test of specimen of RCF3) and the identified strength and stiffness degradation factor (using Bouc-Wen nonlinear hysteresis model is shown in *Figure 13*. It is observed that there is a high correlation between the change of strain and the stiffness/strength. The significant change of block shear strain and axial strain is mainly due to the change of strength degradation. This change is also consistent with the reduction of system fundamental natural frequency identified using recursive ARX model.

3-story Steel Frame

Based the global measurement data (i.e. acceleration measurement) and apply the subspace identification to identify the system natural frequencies of the structure, it is found that the system natural frequencies did not change much even for the structural system subjected to a series of earthquake excitation as shown in Table 2. From the analysis of NDI data of the first floor column, it is observed that after the EQ3 test (with PGA=400 gal) the maximum stress at the top of the first column will reach the yield stress. Based on the ambient vibration data collected from the test specimen after each earthquake excitation, the null-space damage detection algorithm was applied (using global acceleration measurement). *Figure 14* shows the null-space damage index with respect to each test case (white noise excitation). It is observed that a significant increase of the null-space damage index after test case of WN6 (i.e. after the earthquake excitation of EQ4, PGA=570 gal). It demonstrated that the local information identified from the NDI data is close to the global damage information.

CONCLUSIONS

The objective of this research is to analyze the displacement data collected from the multivariate dense light targets through optical tracker from the seismic response of two structures. Through the proposed local structural integrity index (element curvature, element strain and null-space damage index), detail observation and analysis from the NDI data local damage severity can be identified. The optical sensors provided a good

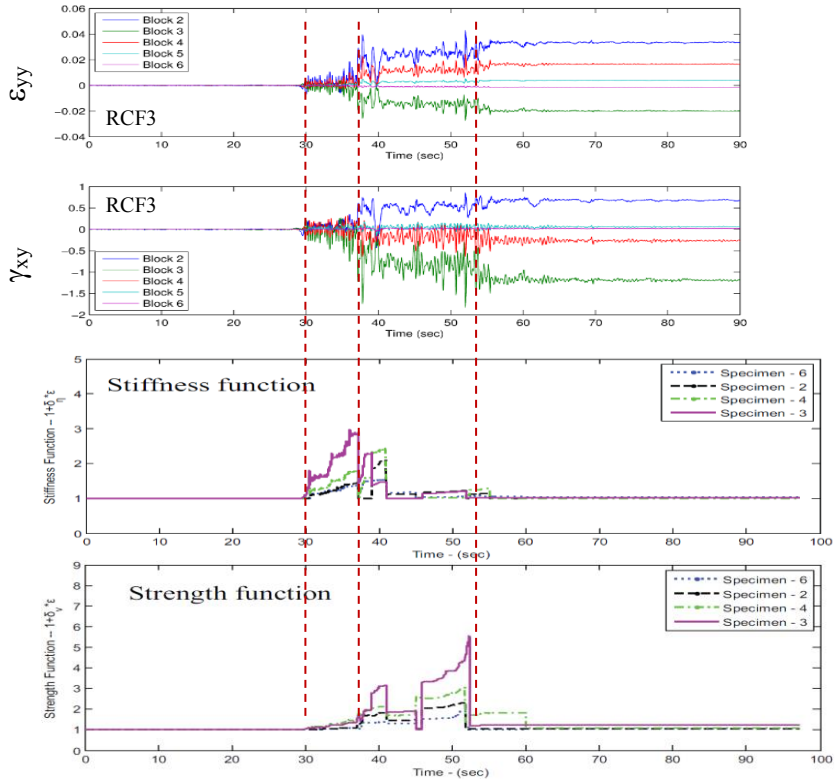

Figure 13 Comparison between the estimate block axial/shear strain and the identified system stiffness/strength degradation

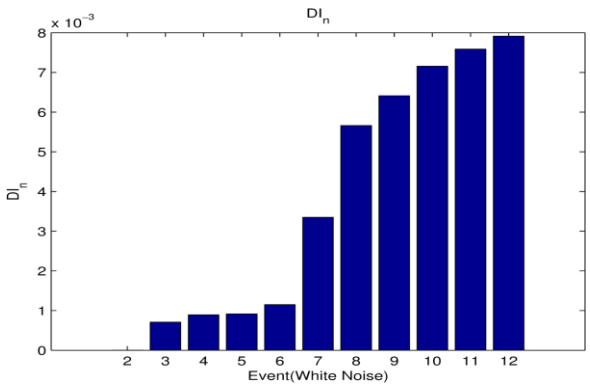

Figure 14 Plot of null-space damage index from different test cases (from white noise excitation) using acceleration response measurement.

ability for recording the local behavior of a structure. Analysis through proper signal processing techniques, physical local feature could be extracted. PCA could be employed to reduce the noise effect on the data and made clearer identification results in strain data. Rigid body motion, which was the 1st PC of the structure, can be also removed. Therefore, the real time history of displacement could be extracted and used to estimate the stress distribution of the element. Besides, a good correlation on the damage features using global information and local measurement can be established.

ACKNOWLEDGEMENTS

The support from Monistry of Science & Technology under grant No. MOST 103-2625-M-002 -006 is acknowledged.

REFERENCES

Boashash, B. (1992). Estimating and Interpreting the Instantaneous Frequency of a Signal. II. Algorithms and Applications. *Proceedings of the IEEE*, **80**(4), page 540-568.

Chao, S.H. and Loh, C.H. (2013). "Vibration-Based Damage Identification of Reinforced Concrete Member Using Optical Sensor Array Data,*" Structural health monitoring* 12(5-6), page 397-410.

Jolliffe, I.T. 2002. *Principal Component Analysis*. volomue. 2nd, Springer.

Loh, C. H**.**, C. H. Mao, J. R. Huang and T. C. Pan (2011), System Identification of Degrading Hysteresis of Reinforced Concrete Frames, *Earthquake Engineering and Structural Dynamics*, 40: page:623–640.

Yan, A.M. and Golinval, J.C. (2006). "Null subspace-based damage detection of structures using vibration measurements." *Mechanical Systems and Signal Processing*, Vol: 20, 611–626.